Molecular Neurobiology (2021) 58:5756–5771
https://doi.org/10.1007/s12035-021-02528-1

ORIGINAL ARTICLE

Effects and Mechanisms of Synaptotagmin-7 in the Hippocampus on Cognitive Impairment in Aging Mice

Yaru Xie[1] · Kaining Zhi[1] · Xianfang Meng[1]

Received: 4 February 2021 / Accepted: 8 August 2021 / Published online: 17 August 2021

Abstract

Aging is an irreversible biological process that involves oxidative stress, neuroinflammation, and apoptosis, and eventually leads to cognitive dysfunction. However, the underlying mechanisms are not fully understood. In this study, we investigated the role and potential mechanisms of Synaptotagmin-7, a calcium membrane transporter in cognitive impairment in aging mice. Our results indicated that Synaptotagmin-7 expression significantly decreased in the hippocampus of D-galactose-induced or naturally aging mice when compared with healthy controls, as detected by western blot and quantitative reverse transcriptase-polymerase chain reaction analysis. Synaptotagmin-7 overexpression in the dorsal CA1 of the hippocampus reversed long-term potentiation and improved hippocampus-dependent spatial learning in D-galactose-induced aging mice. Synaptotagmin-7 overexpression also led to fully preserved learning and memory in 6-month-old mice. Mechanistically, we demonstrated that Synaptotagmin-7 improved learning and memory by elevating the level of fEPSP and downregulating the expression of aging-related genes such as p53 and p16. The results of our study provide new insights into the role of Synaptotagmin-7 in improving neuronal function and overcoming memory impairment caused by aging, suggesting that Synaptotagmin-7 overexpression may be an innovative therapeutic strategy for treating cognitive impairment.

Keyword Synaptotagmin-7; Overexpression; Cognitive impairment; Hippocampus; Long-term potentiation

Introduction

According to the United Nations World Population Forecast, the elderly are projected to constitute 1/4 of the global population by 2050. Population aging has become a major worldwide health and social issue along with the growing amount of elderly people [1–3]. Aging causes irreversible structural and functional degeneration in tissues and cells, which is mainly classified into physiological and pathological senescence. Physiological senescence occurs after maturity, while pathological senescence results from various external factors (including various diseases) [4, 5]. Among various organs, the brain is particularly prone to oxidative stress and apoptosis, due to its limited antioxidant-defense and high metabolic activity and lipid content. Brain aging is a critical risk factor in neurodegenerative diseases [6]. Neurodegeneration refers to the gradual loss of neuronal structure and function, as well as the decline of cognition. Cognitive dysfunction which mainly manifests as one or more disorders in memory, language, calculation, understanding, and judgment, affects the daily life and social communication of elderly people [7–9]. The incidence of Alzheimer's disease (AD) and related neurodegenerative diseases accompanied with aging is also increased.

The hippocampus is a brain region that is sensitive to injury-related factors. Aging impairs the plastic response of the hippocampus to injury. Long-term potentiation (LTP), a key neural mechanism of learning and memory, is impaired in various subregions of the hippocampus with age. Moreover, synaptic plasticity–related genes are downregulated

Highlights
- The expression of Syt7 was decreased in the hippocampus of aging mice.
- Syt7 overexpression in CA1 improved cognitive function of mice.
- Syt7 inhibited senescence by regulating the expression of p16 and p53.
- Syt7 is a valuable target for treating neurodegenerative diseases.

✉ Xianfang Meng
xfmeng@mails.tjmu.edu.cn

[1] Department of Neurobiology, Institute of Brain Research, School of Basic Medical Sciences, Tongji Medical College, Huazhong University of Science and Technology, Wuhan 430030, China

and aging-related genes are induced as the brain ages. Synaptotagmin (Syt) proteins, a type of membrane transport proteins, have tandem C2 domains in the C-terminal and N-terminal transmembrane domains. The Syt protein family includes 17 isoforms, many of which manifest as sensors in the calcium signaling pathway by binding with Ca^{2+} for synaptic transmission [10–12]. Syt7 is widely expressed in different organs and participates in a variety of physiological processes. For example, Syt7 specifically binds soluble N-ethylmaleimide-sensitive fusion protein attachment protein receptor (SNARE) and triggers exocytosis in neurons [13]. Although it has been shown that Syt7 is moderately expressed in many tissues such as the prostate and liver, Syt7 is highly and ubiquitously expressed in the brain [14]. Previous data have revealed that Syt7 mediates facilitation at synapses and plays important role in learning and memory. However, whether and how Syt7 is involved in aging-related cognitive decline is still unclear.

D-galactose (D-gal) was reported to accelerate the brain-aging process in animal models, which is one of the most commonly used methods to investigate the brain-aging process [15–18]. The chronic administration of D-gal to animals can induce brain aging, which is similar to natural aging [19]. D-gal can be metabolized to glucose at normal physiological concentrations and presented in nervous tissue as D-galactosides [20]. However, when the level of D-gal in brain tissue exceeds the normal concentration for a long time, it can be oxidized by galactose oxidase to H_2O_2, and then reacts with Fe^{2+} to form two OH^- molecules. H_2O_2 and OH^- can cause lipid peroxidation of the cell membrane and damage the dynamic balance of redox reactions, thus resulting in neuronal damage [21–24].

However, to date, the role of Syt7 in D-gal-induced and natural aging has not been identified. Thus, in the present study, we aimed to evaluate the effects of Syt7 on learning, memory impairment, and neuronal damage, as well as explore the mechanisms in aging.

Materials and Methods

Animals

All experimental procedures were approved by the Huazhong University of Science and Technology Ethics Committee for Care and Use of Laboratory Animals. Protocols were in accordance with the National Institute of Health Guide for the Care and Use of Laboratory Animals. Eight-week-old male C57BL/6 J mice were purchased from Charles River (Beijing, China) Experimental Animal Technology Co., Ltd., whereas 1-month-old, 2-month-old, 6-month-old, 8-month-old, and 12-month-old mice were purchased from Speifel (Beijing, China) Experimental Animal Technology. The mice were fed in a specific-pathogen free-grade environment, kept in groups of 4 mice per cage and maintained on a 12-h light/dark cycle, and given free access to sufficient food and water.

Experimental Protocol

Preparation of Chronic Aging Animal Models After Syt7 Overexpressed

Male C57BL/6 J mice (8-week-old, 22–25 g) were randomly divided into the following 4 groups and treatment is shown in Scheme 1:

1. AAV9-GFP + control mice were injected with 200 nL of an adeno-associated virus 9 vector expressing green fluorescence protein (AAV9-GFP) in the bilateral CA1. Three weeks later, the mice were injected with normal saline at the back of the neck for 6 weeks.
2. AAV9-GFP + D-gal mice were injected with 200 nL AAV9-GFP in the bilateral CA1. Three weeks later, the mice were injected with D-gal (100 mg/[kg·day]) at the back of the neck for 6 weeks.

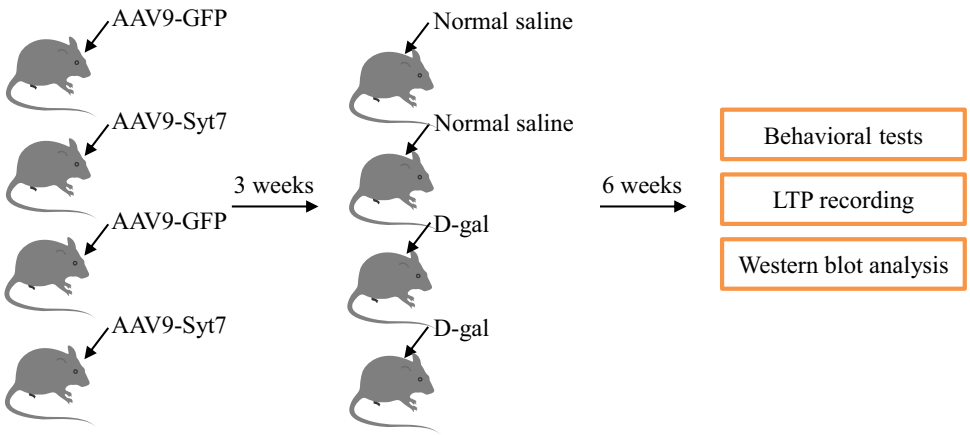

Scheme 1 Preparation of chronic aging animal models after Syt7 overexpressed

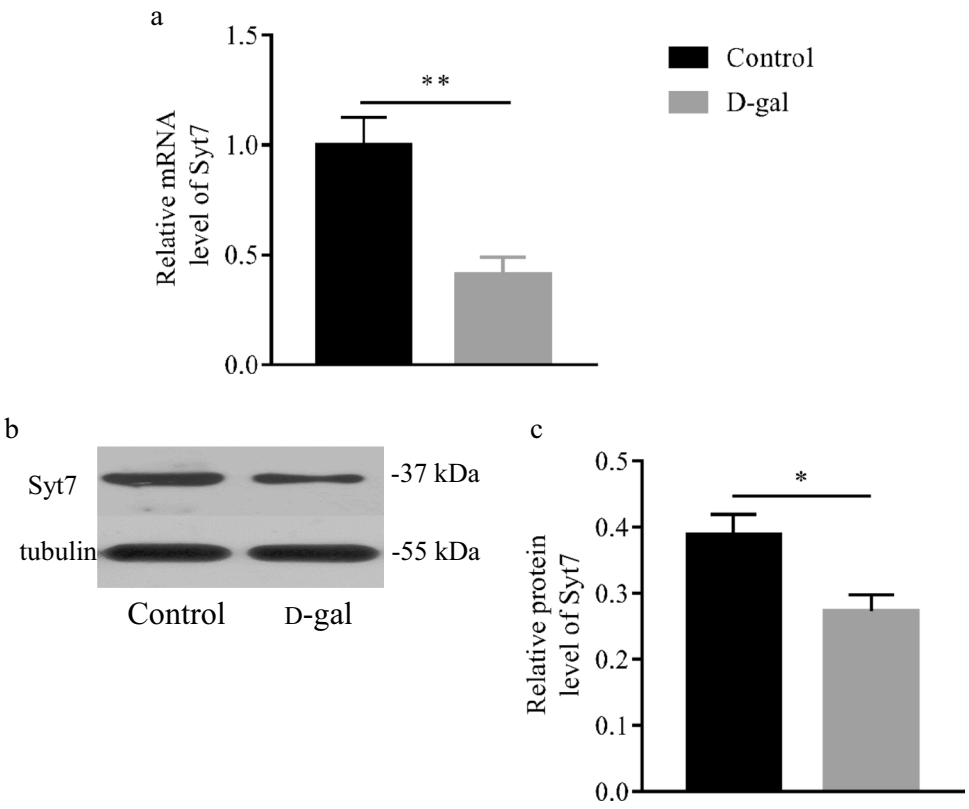

Fig. 1 Syt7 expression decreased in D-gal-induced aging mice. **a** Relative Syt7 mRNA expression levels of the CA1 were detected by qRT-PCR ($n=5$). **b**, **c** Western blot analysis was conducted to measure Syt7 protein expression ($n=3$). All data were presented as the mean ± SEM. ns, not significant ($p>0.05$); *$p<0.05$, **$p<0.01$, ***$p<0.001$, ****$p<0.0001$ vs. the D-gal-induced aging group, based on an unpaired *t* test

3. AAV9-Syt7 + control mice were injected with 200 nL of an AAV9 vector expressing Syt7 (AAV9-Syt7) in the bilateral CA1. Three weeks later, the mice were injected with normal saline at the back of the neck for 6 weeks.
4. AAV9-Syt7 + D-gal mice were injected with 200 nL AAV9-Syt7 in the bilateral CA1. Three weeks later, the mice were injected with D-gal (100 mg/[kg·day]) at the back of the neck for 6 weeks.

Preparation of Animal Models of Overexpressing Syt7 in Aging Mice

Male C57BL/6 J mice (6-month-old) were randomly divided into the following 2 groups:

1. Control group: mice were administered 200 nL AAV9-GFP in the bilateral CA1;
2. Model group: mice were administered 200 nL AAV9-Syt7 in the bilateral CA1.

Behavioral Testing

All behavioral experiments were performed in a double-blind manner. The animals were adapted in the behavior room for 2 h. All behavioral experiments were performed in the same period, and mice in different groups were alternately subjected to the same behavioral experiment which was conducted under quiet conditions. Mice in poor health, such as those with skin lesions, low weight, slow movement, or inability to swim or move, were excluded from behavioral experiment. Besides, all behavioral parameters were monitored through SuperMaze software (Xinruan Information Technology Co. Ltd., Shanghai, China). The software tracked the mice through the computer vision technology of the camera and calculated the difference between each frame, and then, the behavioral data such as the speed, distance, and time of movement were generated.

New Object Recognition Test (NORT)

The NORT experiment was divided into 2 stages:

1. Learning phase: The mice were presented with two identical objects in the NORT chamber and allowed to explore the objects freely for 15 min.
2. Test phase: After 2 h of the learning phase, the mice were exposed to one object used during the learning phase. The other object was replaced by a new object with a different shape and color.

When a mouse touched or sniffed an object within ≤ 2 cm, it was considered exploratory behavior. After each experiment, the box was cleaned with 75% alcohol. The behaviors were recorded and analyzed with the SuperMaze software

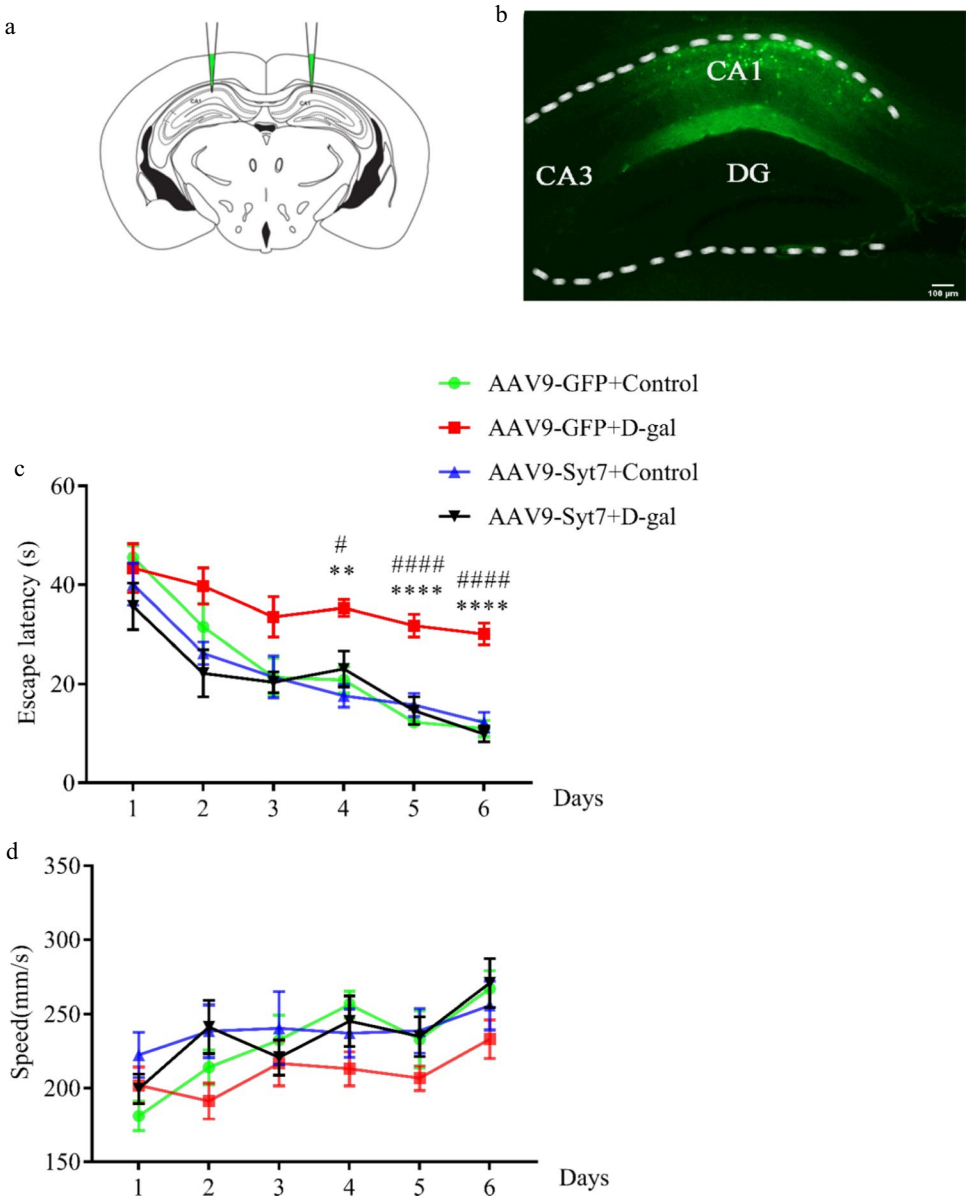

Fig. 2 Effects of Syt7 overexpression in CA1 with D-gal-induced aging mice. Syt7 was overexpressed in the CA1 for 3 weeks, followed by intraperitoneal D-gal injection for 6 weeks. **a** Illustration of bilateral viral vector injections into hippocampal CA1. **b** Representative fluorescence image showing Syt7 expression in CA1 after AAV9-Syt7 vector injection. Scale bar: 100 μm. **c** Latency escape during the acquisition training phase observed in the MWM test. **d** The average swimming speed during the acquisition training phase. **e**–**g** Various indicators observed during the MWM test, including **e** the total distance moved on the platform, **f** the total movement time on the platform, and **g** the number of platform crossing within 1 min. **h** The total time taken to explore the objects. **i** The recognition index of mice for a familiar object versus a novel object at 2 h after familiarization during a 15-min test. **j** Three electric shocks were delivered to the feet of mice at 60-s intervals through a stainless steel grid floor. At the CFC evaluation stage, the animals were exposed to the same equipment for 5 min. **k** Freezing time during the fear-training phase. Contextual fear memory was assessed on the 1st, 3rd, 5th, and 7th days after fear conditioning ($n=8$). All data were presented as the mean ± SEM. ns, not significant ($p>0.05$); *$p<0.05$, **$p<0.01$, ***$p<0.001$, ****$p<0.0001$ vs. the control group, based on two-way ANOVA with an unpaired test. #$p<0.05$, ##$p<0.01$, ###$p<0.001$, ####$p<0.0001$ vs. the AAV9-Syt7 + D-gal group, based on two-way ANOVA with an unpaired test

(Xinruan Information Technology Co. Ltd., Shanghai, China). Recognition index (RI) is defined as follows: RI = (time to explore the new object / total time to explore two objects) × 100%.

Morris Water Maze (MWM) Test

The MWM test involves acquisition training and probe test. During the acquisition training, the platform was hidden

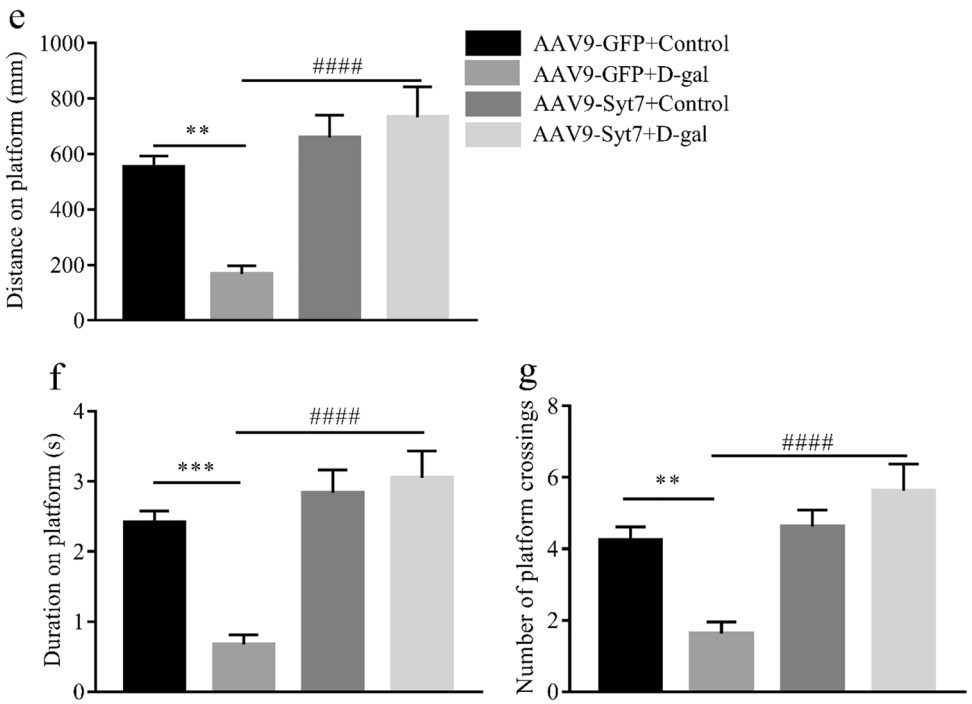

Fig. 2 (continued)

1 cm below the water, and mice were trained to find it with cues guided outside the maze. During every trial, each mouse had 60 s to find the hidden platform; otherwise, it would be guided to the hidden platform, after which it stayed on the platform for 15 s. The trial was conducted 3 times a day for 6 consecutive days with at least 1 h's interval between each trial. On the 7th day, probe test was conducted. The platform was moved away and the animals were allowed to freely swim for 60 s. The behaviors, including the swimming pathway, speed, total distance, and escape latency of mice (to seek hidden platform), were recorded and analyzed using SuperMaze software (Xinruan Information Technology Co. Ltd.).

Contextual Fear Conditioning (CFC) Test

The CFC test was performed in a box equipped with stainless steel grid floor. The SuperMaze software program (Xinruan Information Technology Co., Ltd.) controlled the shock scrambler, which delivered the foot shock through the floor. On the training day, the mice were placed in the CFC box after adapting to the behavioral laboratory environment. After 2 min of adaptation, 3 electric foot shocks (0.7 mA, 5 s) were delivered at intervals of 60 s through stainless steel grid floor, which is referred as the fear-training phase. At the stage of CFC evaluation, the animals were exposed to the same equipment on the 1st, 3rd, 5th, and 7th day for 5 min. The freezing behavior was recorded for each test session using SuperMaze software, and the boxes were cleaned with 75% alcohol.

Hippocampal Slice Preparation and Extracellular Recordings

The mice were deeply anesthetized via 0.3% pentobarbital sodium injection before being euthanized. The brain was quickly removed and submerged in cold aCSF. The composition of aCSF was as follows (mM): 124 NaCl, 3 KCl, 2 $MgCl_2$, 2 $CaCl_2$, 1.25 NaH_2PO_4, 26 $NaHCO_3$, and 10 glucose. The cutting and recording solutions are the same in composition. Then, the brain was dissected, and 310-μm-thick transverse slices were cut from the brain through a vibration slicer (Leica VT1000S, Leica Microsystems, Germany) in ice-cold aCSF bubbled with 95% O_2 and 5% CO_2. Whereafter, the slices were incubated for 30 min in a submerged chamber filled with aCSF bubbled with 95% O_2 and 5% CO_2 at 37℃.

The slices were transferred to a recording chamber. Bipolar nichrome electrodes were used to stimulate the Schaffer collaterals (100 μs, 0.1 Hz) and record the field excitatory postsynaptic potential (fEPSP) in CA1 after stimulation. fEPSPs were collected and analyzed using MED64 Mobius 0.5.0 software in the MED64 planar microelectrode array system, and the minimum amplitude was computed by finding the smallest waveform *y*-value between the cursors. The system noise was controlled to ± 5 μV. The setting of the

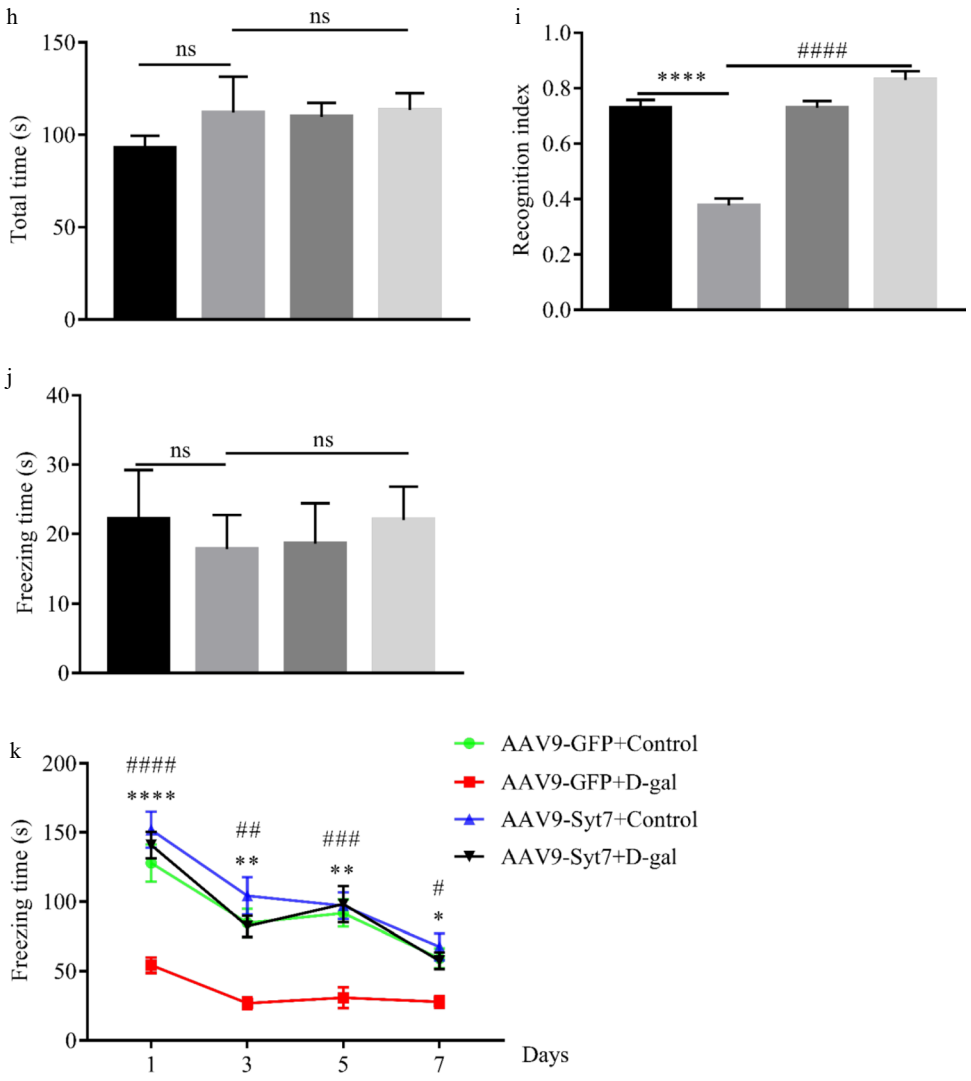

Fig. 2 (continued)

stimulus intensity should consider not only the increase of LTP but also the enlargement of fEPSP as much as possible to reduce the interference of environmental factors on the waveform of fEPSP. The stimulus intensity calculated by our formula is 30–50% of the maximum amplitude. Therefore, the appropriate stimulus intensity was selected based on the following formula: (maximum amplitude − minimum amplitude) × 35% + the minimum amplitude, in accordance with the input/output curve. The fEPSP was recorded at least 20 min with a stimulation frequency of 0.1 Hz as the baseline. Subsequently, high-frequency stimulation (HFS), consisting of 3 consecutive 100-Hz stimulations separated by 10 s, was applied to elicit LTP. At the same time, the population spikes can be monitored. Successful induction of LTP means that the fEPSP increased at least 20%, and lasted not less than 1 h after HFS stimulation.

Reverse Transcription Quantitative PCR (qRT-PCR) Analysis

The tissues taken from CA1 were prepared for qRT-PCR. A cDNA synthesis kit (Vazyme, Jiangsu, China) was used for reverse transcription, according to the manufacturer's instructions. First, 4 μL 4 × gDNA wiper mix and 1 μg total RNA were transferred to an RNase-free centrifuge tube, diluted with RNase-free H_2O (ddH_2O) to 16 μL, mixed gently with a pipette, and incubated at 42 °C for 2 min to remove genomic DNA. Next, 4 μL 5 × HiScript III qRT SuperMix was added to the mixture, and reverse transcription was performed.

The specific primers were designed and synthesized by Sangon Biotech (Sangon Biotech Co. Ltd., Shanghai, China). Primers specific for mouse Syt7 were 5′-CGGGTTCTGAGG AGGATG-3′ and 5′-TTTGTGCTTCTTGTCGGG-3′; primers specific for β-actin were 5′-TTTGTGCTTCTTGTCGGG-3′

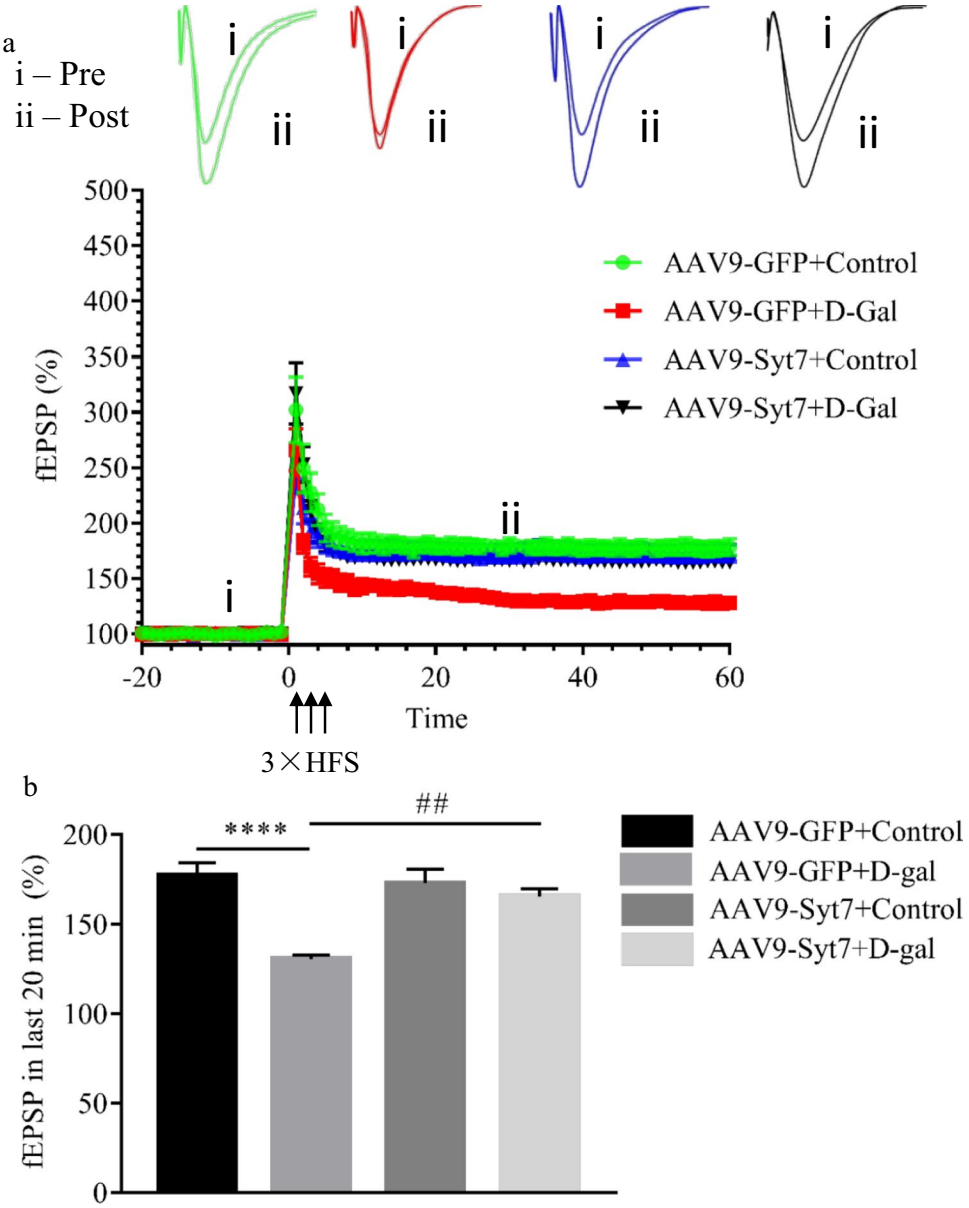

Fig. 3 LTP decay induced by D-gal was abolished by Syt7 overexpression. **a** Average amplitude of LTP induced by 3×HFS. Top, sample traces taken at time points (i) and (ii) indicated above the summary plots. **b** The mean fEPSP during the last 20 min in acute brain slices from control mice or mice subjected to D-gal-induced aging plus injection with AAV9-Syt7 or AAV9-GFP ($n=15$; slices obtained from 4 to 5 mice). All data were presented as the mean ± SEM. ns, not significant ($p>0.05$); *$p<0.05$, **$p<0.01$, ***$p<0.001$, ****$p<0.0001$ vs. the control group, based on two-way ANOVA with an unpaired test. #$p<0.05$, ##$p<0.01$, ###$p<0.001$, ####$p<0.0001$ vs. the AAV9-Syt7 + D-gal group, based on two-way ANOVA with an unpaired test

and 5′-TCACGGTTGGCCTTAGGGTT-3′. The reaction solution of qPCR was prepared according to the manufacturer's instructions of ChamQ SYBR qPCR Master Mix (Vazyme). Each sample was placed in ABI StepOnePlus qPCR instrument and a thermocycling program was initiated. The relative mRNA-transcript level was determined by ΔΔCt method.

Western Blot Analysis

Western blot analyses were conducted as previously described [25]. The tissues taken from CA1 were lysed by RIPA (Beyotime, Shanghai, China), and the protein concentration was detected using a BCA Protein Assay Kit (Beyotime, Shanghai, China) according to the manufacturers' instructions. Proteins were normalized to 60 μg/lane, separated on polyacrylamide gels, and then electrophoretically transferred to 0.22 μm polyvinylidene fluoride membranes (Merck Millipore, MA, USA). The membranes were incubated with Tris-buffered saline with Tween-20 (TBST) containing 5% skim milk for 1 h at room temperature to block nonspecific protein binding. Subsequently, the membranes were incubated with the following antibodies: CDKN2A/p16INK4a (1:1000; Abcam, Cambridge, MA, USA), GFP (1:1000, ProteinTech Group, Inc., Wuhan, China), Syt7 (1:1000, Sigma-Aldrich Co.), P53 (1:1000, ProteinTech Group, Inc.), α-tubulin (1:1000, ProteinTech Group, Inc.) at 4℃ overnight. Then, the membranes were hybridized with horseradish peroxidase–conjugated secondary antibody (1:10,000, AntGene, Wuhan, China) for 1 h at room temperature. Afterwards, the protein bands were detected with ECL

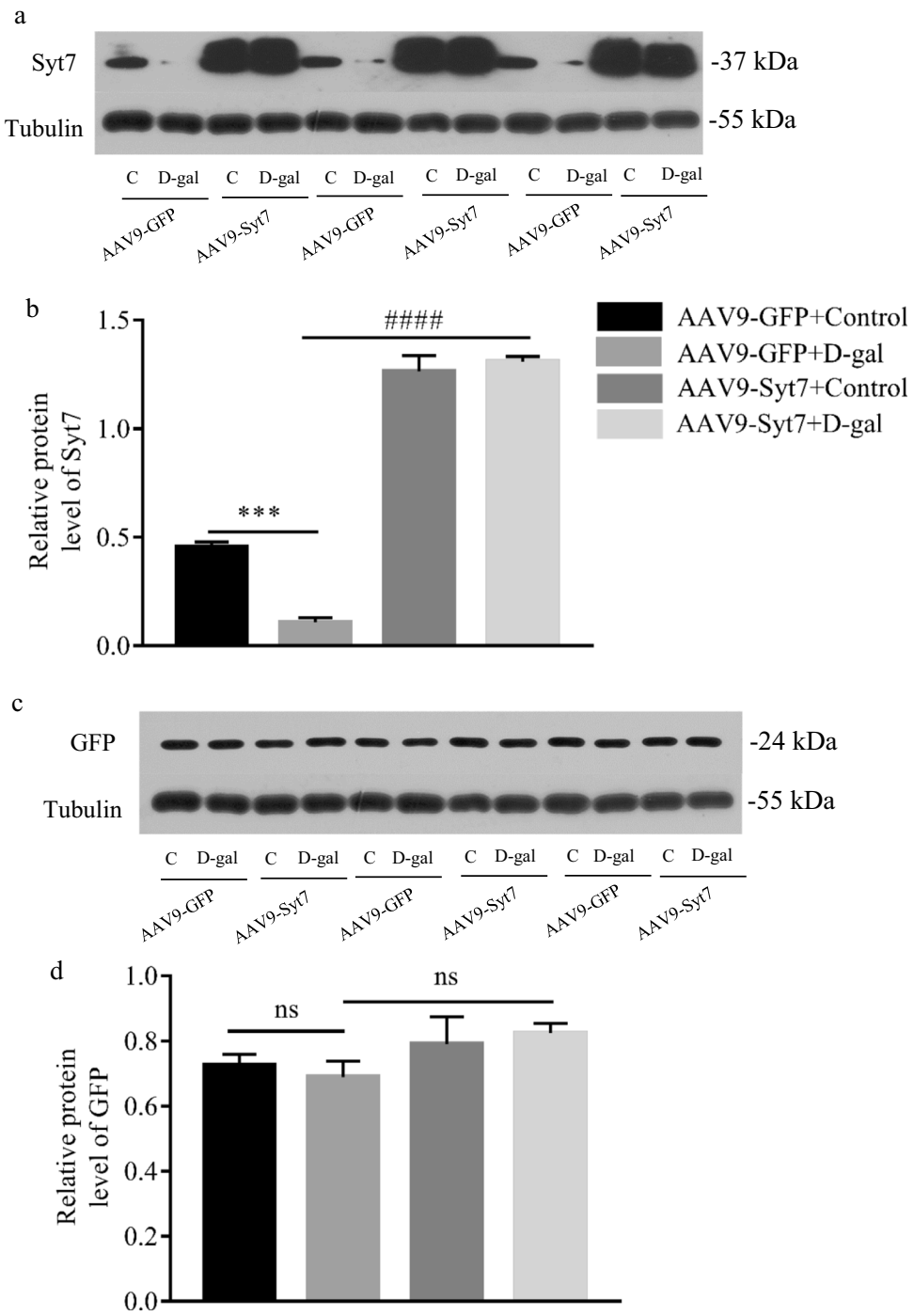

Fig. 4 Syt7 inhibited hippocampus senescence by downregulating p16 and p53 expression. **a**–**d** Expression of Syt7 (**a**, **b**) and GFP (**c**, **d**) in the CA1 of each group of mice and representative western blot figures. **e**–**h** Quantification and representative western blots of the aging-related proteins p53 (**e**, **f**) and p16 (**g**, **h**) in the hippocampal CA1 of mice ($n=3$). All data were presented as the mean ± SEM. ns, not significant ($p>0.05$); *$p<0.05$, **$p<0.01$, ***$p<0.001$, ****$p<0.0001$ vs. the control group, based on two-way ANOVA with an unpaired test. #$p<0.05$, ##$p<0.01$, ###$p<0.001$, ####$p<0.0001$ vs. the AAV9-Syt7 + D-gal group, based on two-way ANOVA with an unpaired test

(Epizyme Biotech, Shanghai, China) chemiluminescence substrate. The results were analyzed by ImageJ software (National Institutes of Health, Bethesda, MD, USA).

Animal Surgery and Stereotactic Viral Injection

The mice were deeply anesthetized via intraperitoneal injection of 0.3% pentobarbital sodium. Hair on the surgical area was shaved, the surgical area was sterilized with iodophor solution, and vaseline was applied to keep the eyes moist. Next, each mouse was placed on a stereotaxic apparatus (68,030, RWD Life Science, China). Small holes were made above the CA1 (AP − 2.7 mm, ML ± 2 mm, DV + 1.68 mm from the bregma) by drilling into the skull. AAV9-Syt7 or AAV9-GFP was injected through a beveled glass micropipette backfilled with mineral oil. The flow rate (20 nL/min)

Fig. 4 (continued)

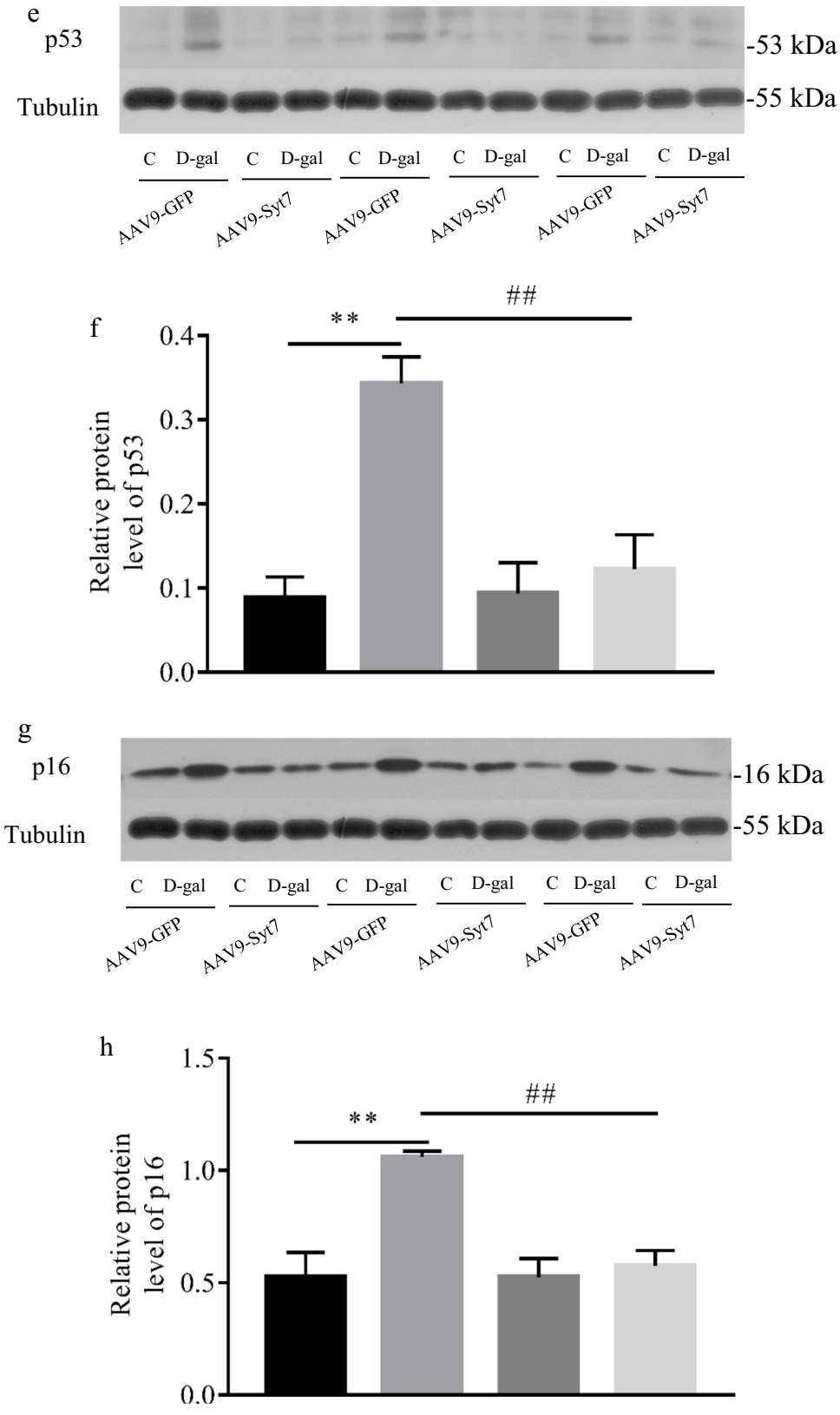

was kept constant using a syringe pump. The micropipette was maintained for at least 10 min after the injection and removed slowly. Then, the wound was stitched and normal saline was injected subcutaneously.

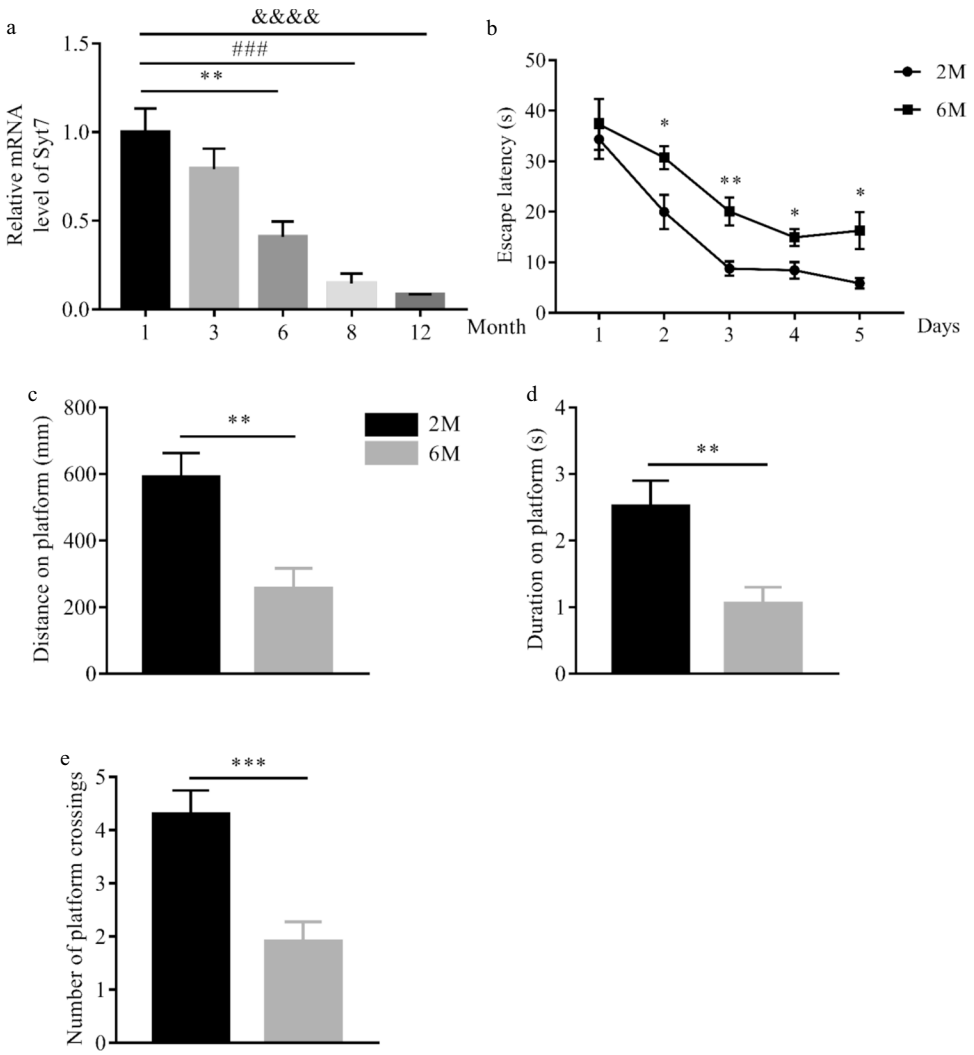

Fig. 5 Hippocampus-related learning and memory were impaired in 6-month-old mice. **a** Relative Syt7 mRNA expression of CA1 in mice of different ages, ranging from 1 to 12 months old ($n=3$). **b** Learning curves from the MWM test during acquisition training ($n=10$). **c**–**e** Total swim distance (**c**) and total swim time (**d**) on the platform, and the number of platform crossing within 1 min (**e**) ($n=10$). All data were presented as the mean ± SEM. ns, not significant ($p>0.05$); *$p<0.05$, **$p<0.01$, ***$p<0.001$, ****$p<0.0001$ vs. 2-month-old mice, based on an unpaired *t* test

Statistics

The experimental data were expressed as the mean ± standard error of the mean (SEM) and analyzed by two-way analysis of variance (ANOVA) or *t* test in GraphPad Prism (version 7.0). $p<0.05$ was considered to reflect a statistically significant difference.

Results

Syt7 Expression Decreased in D-gal-Induced Aging Mice

To elucidate whether Syt7 is involved in aging-related cognitive impairment, we first detected Syt7 expression in CA1 of the hippocampus of D-gal-induced aging and control mice by qRT-PCR and western blotting analysis. We found lower mRNA and protein expression of Syt7 in the CA1 of aging mice compared with controls (Fig. 1a–c).

Syt7 Overexpression in CA1 Improved Impaired Hippocampus-Dependent Learning and Memory in D-gal-Induced Aging Mice

To further explore the role of Syt7 in cognition, we investigated whether overexpressing Syt7 in the hippocampus of C57BL/6 J mice would ameliorate aging-related cognitive impairment. AAV9-Syt7 or AAV9-GFP was delivered specifically to the bilateral CA1 of the hippocampus by stereotactic injection (Fig. 2a, b). After 3 weeks, the mice were subcutaneously injected with D-gal or normal saline at the back of the neck for 6 weeks. First, the spatial learning and memory of the mice were detected by MWM tests [26, 27]. The results indicated that during the training period, Syt7 overexpression improved learning in D-gal-treated mice (Fig. 2c). However, no significant difference was found in the average swimming speed among the 4 groups (Fig. 2d). On the 7th day, we removed the platform to assess the spatial memory. In D-gal-treated mice, AAV9-Syt7 injection increases the distance and time spent in target platform

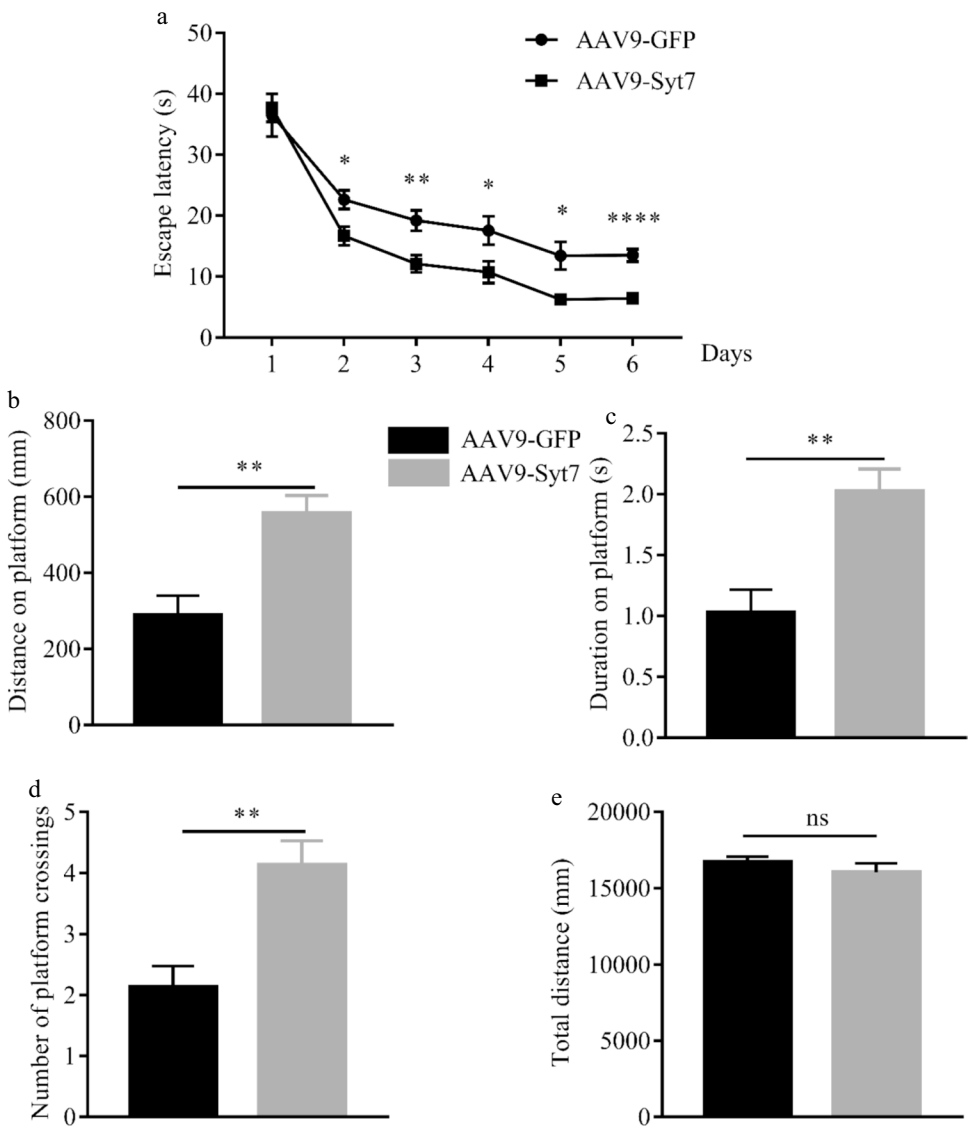

Fig. 6 Effects of Syt7 overexpression in CA1 of aging mice. **a** The AAV9-Syt7 or AAV9-GFP vector was injected in the bilateral CA1 in 6-month-old mice after the measurement of escape latency to the platform during acquisition training in the MWM test. **b–e** Total swim distance on the platform (**b**), total swim time on the platform (**c**), the number of platform crossing within 1 min (**d**), and total swim distance in the MWM during the probe test (**e**). **f** The total time taken to explore the objects. **g** The preference of mice for a familiar object and a novel object at 2 h after familiarization during a 15-min test. **h** Freezing time during training phase in the CFC test. **i**, **j** Freezing time related to contextual fear memory assessed on the 1st (i) and the 3rd (j) days after fear conditioning ($n = 8$). All data were presented as the mean ± SEM. ns, not significant ($p > 0.05$); *$p < 0.05$, **$p < 0.01$, ***$p < 0.001$, ****$p < 0.0001$ vs. the AAV9-GFP group, based on an unpaired *t* test

location than controls (Fig. 2e–g), suggesting that Syt7 overexpression enhanced spatial memory.

Then, we performed NORT to evaluate object recognition memory [28, 29]. By analyzing the total time to explore two objects and RI, we found that there was no significant difference in the total time spent exploring two objects (Fig. 2h). In AAV9-GFP-injected groups, aging mice had a lower preference for exploring the new object than controls. However, Syt7-overexpressed aging mice showed a stronger desire for new object than aging mice without Syt7 overexpression (Fig. 2i).

Besides, we used CFC test to further evaluate hippocampus-dependent learning and memory in mice [30]. The mice showed similar freezing time during foot shock phase (Fig. 2j). However, in the contextual fear conditioning paradigm, aging mice with Syt7 overexpression showed significantly enhanced freezing behavior at day 1, day 3, day 5, and day 7 after training, compared to aging mice without Syt7 overexpression (Fig. 2k).

In addition, we found that Syt7 overexpression in CA1 does not affect depressive- and anxiety-like behavior and spontaneous motor activity in aging mice (Supplementary Fig. 1).

Syt7 Overexpression Enhanced Hippocampal Long-Term Potentiation

LTP is one of the major methods used to explain learning and memory [31]. To test whether Syt7 modulates long-term synaptic plasticity, we detected LTP levels, which were induced by 3 × HFS at Schaffer collateral-CA1 synapses in slices. LTP decreased significantly after 3 × HFS induction, and the fEPSP amplitude decreased during the last 20 min in the AAV9-GFP-injected aging group, compared to the AAV9-GFP-injected control group. However,

Fig. 6 (continued)

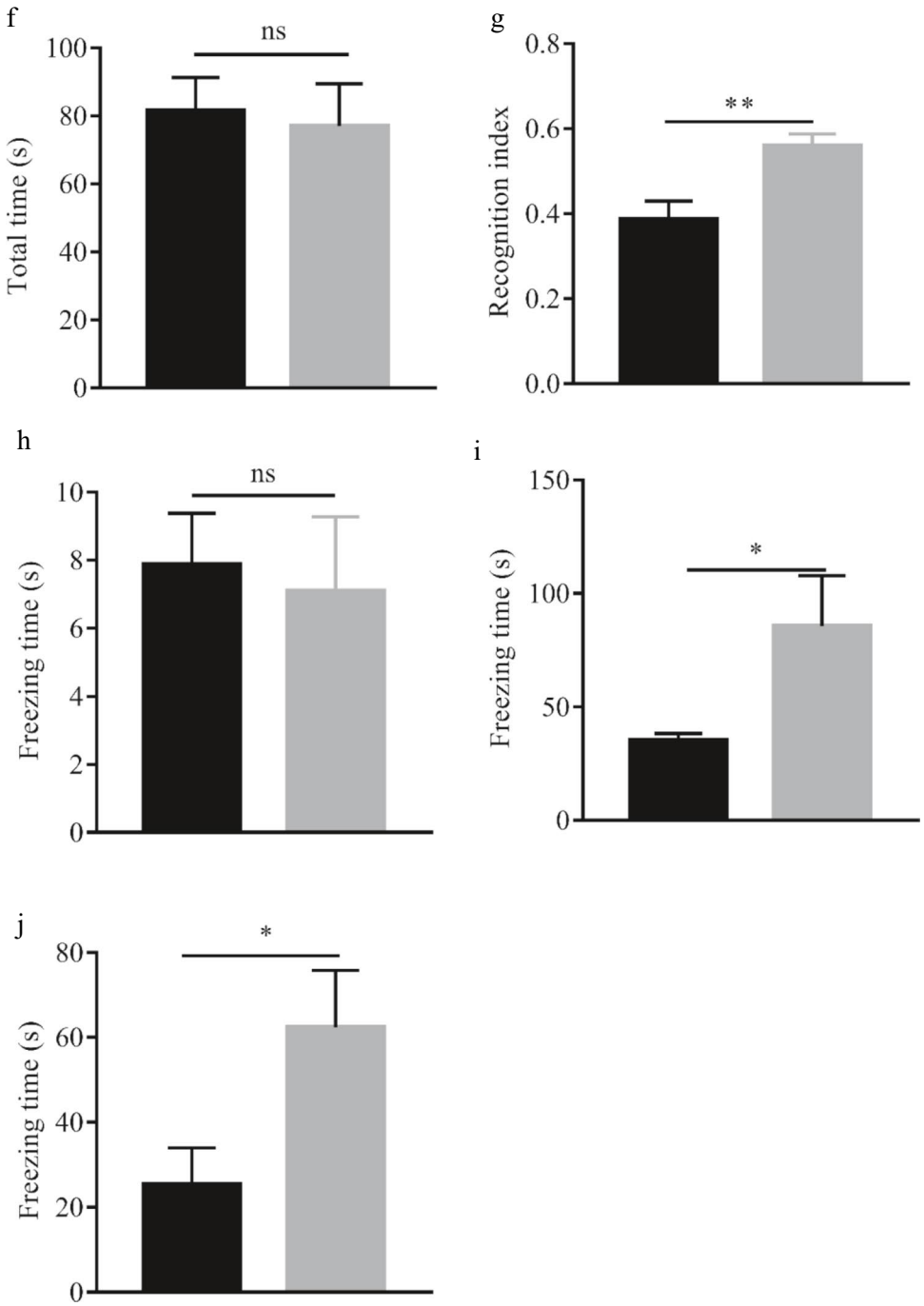

Syt7 overexpression in CA1 reversed hippocampal LTP deficiency in D-gal-induced aging mice (Fig. 3a, b).

Syt7 Inhibited Senescence in the Hippocampus by Downregulating the p16 and p53 Expression

To further elucidate the mechanisms of Syt7 in senescence, we detected the level of Syt7 in CA1 of the mice mentioned above. We found that the expression of Syt7 decreased in D-gal mice, but increased sharply in the CA1 of Syt7-overexpressing mice (Fig. 4a, b). The level of GFP was similar among all groups (Fig. 4c, d). D-Gal increased the protein levels of p16 and p53 in hippocampal CA1, which was eliminated by the overexpression of Syt7 (Fig. 4e–h).

Overexpression of Syt7 Improved Learning and Memory in Naturally Aging Mice

To clarify whether Syt7 plays an important role in learning and memory of naturally aging mice, we detected

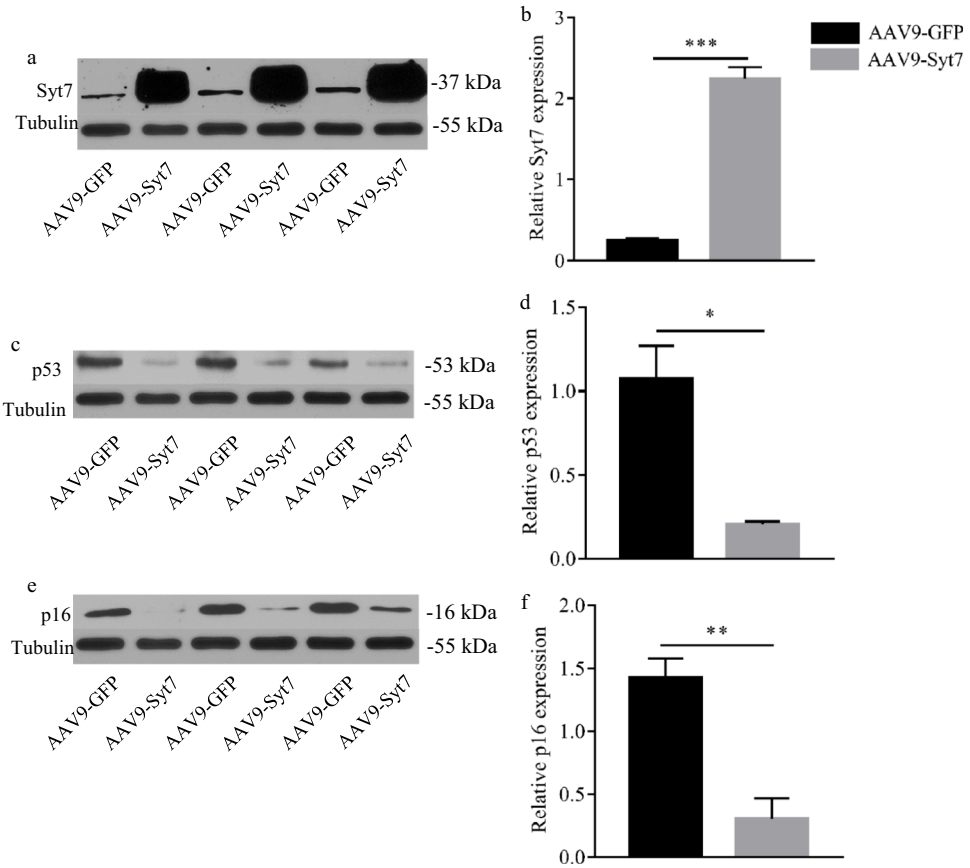

Fig. 7 Syt7 overexpression in CA1 inhibited senescence in naturally aging mice. Protein samples were extracted from the CA1 of the hippocampus in AAV9-GFP- and AAV9-Syt7-injected mice. **a**, **b** representative western blot (**a**) and the relative protein expression levels of Syt7 (**b**) in each group were shown ($n=3$). **c**–**f** Representative western blots and protein levels of p53 (**c**, **d**) and p16 (**e**, **f**) in the CA1 ($n=3$). All data were presented as the mean ± SEM. ns, not significant ($p>0.05$); *$p<0.05$, **$p<0.01$, ***$p<0.001$, ****$p<0.0001$ vs. the AAV9-GFP group, based on an unpaired *t* test

Syt7 expression in CA1 at different ages by qRT-PCR. We found that Syt7 was highly expressed in 1-month-old mice and decreased with age, especially in 6-month-old mice (Fig. 5a). We speculated that 6-month-old mice began to show signs of aging. Thus, we assessed the spatial learning and memory of 2-month-old mice and 6-month-old mice, based on the MWM test. We found that the latent periods in both groups gradually shortened during 5 days of training. From the 2nd day of acquisition training, 6-month-old mice displayed a poor ability to find the hidden platform (Fig. 5b). In comparison with 2-month-old mice, 6-month-old mice showed declined memory in the probe test conducted 5 days after training (Fig. 5c–e). These results suggested that spatial learning and memory were disrupted in 6-month-old mice.

Based on the above results, we delivered AAV9-Syt7 or AAV9-GFP specifically to CA1 in 6-month-old mice by bilateral stereotactic injection, resulting in a selective gene overexpression in CA1. Through a series of behavior tests, we found that Syt7 overexpression in CA1 of hippocampus in 6-month-old mice rescued the poor learning and memory performances in the MWM tests (Fig. 6a–e), strengthened the object recognition ability in the NORT (Fig. 6f, g), and enhanced contextual fear memory (Fig. 6h–j), but did not affect sucrose preference (Supplementary Fig. 2a–c), immobility % in TST (Supplementary Fig. 2d), anxiety-like behavior (Supplementary Fig. 2e, f), and spontaneous motor ability (Supplementary Fig. 2 g), suggesting that Syt7 overexpression can help to improve learning and memory in naturally aging mice. Finally, we verified the Syt7 overexpression in CA1 after AAV9-Syt7 injection and found that the expression levels of senescence-related molecules, p53 and p16, were reversed by Syt7 overexpression (Fig. 7).

Discussion

Syt7, a member of the synaptotagmin gene family, encodes a transmembrane protein that binds Ca^{2+} during synaptic transmission to mediate membrane trafficking [10–12]. Syt7 is widely expressed in various types of biological tissues and plays a vital role in various physiological processes [32]. For example, Syt7 can interact with SNARE protein to regulate the fusion of vesicle and cell membranes, which triggers neuronal cell exocytosis [33, 34]. Syt7 is associated with apoptosis [35], but its role in apoptosis remains unknown. Although many studies have focused on Syt7, the role of Syt7 in cognitive decline during aging still needs to be further elucidate.

Impaired learning and memory has been identified as a sign of aging [36]. We have shown that chronic systemic D-gal

injection can lead to a deficit of learning and memory, and decreased antioxidant enzyme activity, which induces neurodegeneration and aging. Syt7 decreased in D-gal-induced aging mice, which was detected by qRT-PCR and western blotting analysis, confirming the central hypothesis of our study.

Subsequently, we delivered AAV9-Syt7 to the bilateral CA1 of the hippocampus in 8-week-old mice, which were administered D-gal at a dose of 100 mg (/kg·day) at the back of the neck for 6 weeks. Then, we conducted a series of behavior tests such as MWM, NORT, and CFC tests to assess hippocampus-dependent learning and memory in D-gal-treated mice [37–39]. Our results showed that Syt7 overexpression significantly rescued the impaired behaviors in aging mice. For example, Syt7 overexpression reduced the latent period, improved the time spent and distance moved on the hidden platform, increased the times in crossing the platform, and enhanced the object recognition memory and contextual fear memory. These results indicate that Syt7 can relieve cognitive deficiency induced by aging.

To further explore the senescence-related mechanisms of Syt7, we detected the expression of p16 (p16INK4a, cyclin-dependent kinase inhibitor 2A, isoform INK4a) which is the senescence marker and an indicator of irreversible growth arrest (senescence) in cultured cells and tissues. Selective elimination of p16-positive cells can prevent or delay senescent deterioration. Cellular senescence, a process that imposes permanent proliferative arrest on cells in response to various stressors, has emerged as a potentially important contributor to aging and age-related diseases, as well as an attractive target for therapeutic exploitation [4]. Recent findings suggest that senescence also occurs in post-mitotic cells, such as neurons. It has been reported that the activity of senescence-associated beta-galactosidase (SA-β-gal) was increased in post-mitotic neurons of long-term primary cultures (an in vitro model system for studying aging) as well as in the hippocampus of aging mice and rats. Primary rat hippocampal neurons in long-term cultures have shown changes of SA-β-gal and p16, and loss of lamin B1. Moreover, p53, p21, and retinoblastoma protein (Rb) have also been recognized as major regulators of cell senescence. In the present study, we found that D-gal increased p16 and p53 expression in hippocampus, which was consistent with previous studies. Syt7 can inhibit senescence and promote the tumorigenicity of lung cancer cells [40]. However, whether Syt7 overexpression affects the levels of p53 and p16 in the hippocampus remains unknown, our findings indicate that Syt7 overexpression prevents the expression of p53 and p16.

It has been reported that overexpression of Syt7 enhances the binding of MDM2 and p53, resulting in the downregulation of p53 [40]. Therefore, we speculate that Syt7 in CA1 of hippocampus can reduce the expression of p53 by regulating the expression of MDM2.

The hippocampus is a key brain region relevant to cognitive function. Specifically, the CA1 in the hippocampus is the foremost encephalic region for learning and memory [41, 42]. Memory is encoded by synaptic plasticity. As a type of synaptic plasticity, LTP is indispensable for learning and memory [43]. Therefore, LTP in CA1 is widely used to test learning and memory. Here we showed that long-term D-gal administration impaired LTP induction in CA1 and reduced the amplitude of fEPSP. These phenomena could be reversed by Syt7 upregulation.

To further elucidate whether Syt7 also plays a profound role in naturally aging mice, we detected the expression of Syt7 by qRT-PCR in hippocampal CA1 at different ages. We found that Syt7 expression decreased gradually with age, with a sharp decline at 6 months of age. Therefore, we speculate that Syt7 overexpression can alleviate cognitive dysfunction during natural aging.

At present, no relevant literature has been published regarding the specific timing of mouse aging. Our experiments confirmed that Syt7 expression decreased with age. Hippocampal Syt7 expression was markedly lower in 6-month-old mice than in 1-month-old mice. Based on the above results, we hypothesized that the mice might start aging at 6 months of age. Therefore, we performed the MWM test at the age of 2 months and 6 months, and found that the learning and memory were impaired in 6-month-old mice, which was in line with our hypothesis. Based on the abovementioned facts, we injected the AAV9-Syt7 vector into the CA1 of 6-month-old mice and conducted a series of behavioral tests. One of the most interesting findings was that Syt7 overexpression did not cause depression and anxiety or affect the motor abilities of mice, but restored the learning and memory of naturally aging mice. In addition, the protein levels of p53 and p16 were downregulated by Syt7 overexpression, indicating that Syt7 inhibits senescence in naturally aging mice.

In conclusion, our research was the first study to explore the expression of Syt7 in CA1 of aging mice. Moreover, we elucidated the effects and mechanisms of Syt7 overexpression in CA1 of the hippocampus on cognition related to aging. Further researches exploring the function of Syt7 in natural aging and neurodegenerative disease–associated cognitive dysfunction are needed, which may provide prospective targets and new therapeutic regimens for neurodegenerative diseases.

Supplementary Information The online version contains supplementary material available at https://doi.org/10.1007/s12035-021-02528-1.

Acknowledgements We are grateful to Dr. Anni Jiang and Dr. Yuting Zhu for language modification.

Author contribution Yaru Xie and Xianfang Meng performed the experiments; Kaining Zhi analyzed the data; Xianfang Meng designed and supervised the study. All authors wrote the manuscript.

Funding This work was supported by grants from the National Natural Science Foundation of China (grant numbers 81471490, 81671066, and 81974162).

Data availability The datasets generated and/or analyzed during the current study are available from the corresponding author on reasonable request.

Declarations

Ethics approval All experimental procedures were reviewed and approved by the Huazhong University of Science and Technology Ethics Committee for Care and Use of Laboratory Animals.

Consent to participate Not applicable.

Consent for publication Not applicable.

Conflict of interest The authors declare no competing interests.

References

1. Petersen RC, Yaffe K (2020) Issues and questions surrounding screening for cognitive impairment in older patients. JAMA 323(8):722–724. https://doi.org/10.1001/jama.2019.22527
2. Iadecola C, Duering M, Hachinski V, Joutel A, Pendlebury ST, Schneider JA, Dichgans M (2019) Vascular cognitive impairment and dementia: JACC Scientific Expert Panel. J Am Coll Cardiol 73(25):3326–3344. https://doi.org/10.1016/j.jacc.2019.04.034
3. Wyss-Coray T (2016) Ageing, neurodegeneration and brain rejuvenation. Nature 539(7628):180–186. https://doi.org/10.1038/nature20411
4. Guo Y, Li H, Ke X, Deng M, Wu Z, Cai Y, Afewerky HK, Zhang X, Pei L, Lu Y (2019) Degradation of caytaxin causes learning and memory deficits via activation of DAPK1 in aging. Mol Neurobiol 56(5):3368–3379. https://doi.org/10.1007/s12035-018-1312-5
5. Campos PB, Paulsen BS, Rehen SK (2014) Accelerating neuronal aging in in vitro model brain disorders: a focus on reactive oxygen species. Front Aging Neurosci 6:292. https://doi.org/10.3389/fnagi.2014.00292
6. Bauerlein FJB, Fernandez-Busnadiego R, Baumeister W (2020) Investigating the structure of neurotoxic protein aggregates inside cells. Trends Cell Biol. https://doi.org/10.1016/j.tcb.2020.08.007
7. Baller EB, Kaczkurkin AN, Sotiras A, Adebimpe A, Bassett DS, Calkins ME, Chand G, Cui Z, Gur RE, Gur RC, Linn KA, Moore T, Roalf DR, Varol E, Wolf DH, Xia CH, Davatzikos C, Satterthwaite TD (2020) Neurocognitive and functional heterogeneity in depressed youth. Neuropsychopharmacology. https://doi.org/10.1038/s41386-020-00871-w
8. Brai E, Hummel T, Alberi L (2020) Smell, an underrated early biomarker for brain aging. Front Neurosci 14:792. https://doi.org/10.3389/fnins.2020.00792
9. Pei H, Ma L, Cao Y, Wang F, Li Z, Liu N, Liu M, Wei Y, Li H (2020) Traditional Chinese medicine for Alzheimer's disease and other cognitive impairment: a review. Am J Chin Med 48(3):487–511. https://doi.org/10.1142/S0192415X20500251
10. Bowers MR, Reist NE (2020) Synaptotagmin: mechanisms of an electrostatic switch. Neurosci Lett 722:134834. https://doi.org/10.1016/j.neulet.2020.134834
11. Bowers MR, Reist NE (2020) The C2A domain of synaptotagmin is an essential component of the calcium sensor for synaptic transmission. PLoS ONE 15(2):e0228348. https://doi.org/10.1371/journal.pone.0228348
12. Colom-Cadena M, Spires-Jones T, Zetterberg H, Blennow K, Caggiano A, DeKosky ST, Fillit H, Harrison JE, Schneider LS, Scheltens P, de Haan W, Grundman M, van Dyck CH, Izzo NJ, Catalano SM, Working SHE, G, (2020) The clinical promise of biomarkers of synapse damage or loss in Alzheimer's disease. Alzheimers Res Ther 12(1):21. https://doi.org/10.1186/s13195-020-00588-4
13. Zhang J, He J, Johnson JL, Napolitano G, Ramadass M, Rahman F, Catz SD (2019) Cross-regulation of defective endolysosome trafficking and enhanced autophagy through TFEB in UNC13D deficiency. Autophagy 15(10):1738–1756. https://doi.org/10.1080/15548627.2019.1596475
14. Xiao B, Li J, Fan Y, Ye M, Lv S, Xu B, Chai Y, Zhou Z, Wu M, Zhu X (2017) Downregulation of SYT7 inhibits glioblastoma growth by promoting cellular apoptosis. Mol Med Rep 16(6):9017–9022. https://doi.org/10.3892/mmr.2017.7723
15. Ali T, Badshah H, Kim TH, Kim MO (2015) Melatonin attenuates D-galactose-induced memory impairment, neuroinflammation and neurodegeneration via RAGE/NF-K B/JNK signaling pathway in aging mouse model. J Pineal Res 58(1):71–85. https://doi.org/10.1111/jpi.12194
16. Yoo DY, Kim W, Lee CH, Shin BN, Nam SM, Choi JH, Won MH, Yoon YS, Hwang IK (2012) Melatonin improves D-galactose-induced aging effects on behavior, neurogenesis, and lipid peroxidation in the mouse dentate gyrus via increasing pCREB expression. J Pineal Res 52(1):21–28. https://doi.org/10.1111/j.1600-079X.2011.00912.x
17. Li L, Chen B, Zhu R, Li R, Tian Y, Liu C, Jia Q, Wang L, Tang J, Zhao D, Mo F, Liu Y, Li Y, Orekhov AN, Bromme D, Zhang D, Gao S (2019) Fructus Ligustri Lucidi preserves bone quality through the regulation of gut microbiota diversity, oxidative stress, TMAO and Sirt6 levels in aging mice. Aging (Albany NY) 11(21):9348–9368. https://doi.org/10.18632/aging.102376
18. Huang JL, Yu C, Su M, Yang SM, Zhang F, Chen YY, Liu JY, Jiang YF, Zhong ZG, Wu DP (2019) Probucol, a "non-statin" cholesterol-lowering drug, ameliorates D-galactose induced cognitive deficits by alleviating oxidative stress via Keap1/Nrf2 signaling pathway in mice. Aging (Albany NY) 11(19):8542–8555. https://doi.org/10.18632/aging.102337
19. Lu J, Wu DM, Zheng YL, Hu B, Zhang ZF, Ye Q, Liu CM, Shan Q, Wang YJ (2010) Ursolic acid attenuates D-galactose-induced inflammatory response in mouse prefrontal cortex through inhibiting AGEs/RAGE/NF-kappaB pathway activation. Cereb Cortex 20(11):2540–2548. https://doi.org/10.1093/cercor/bhq002
20. Bo-Htay C, Palee S, Apaijai N, Chattipakorn SC, Chattipakorn N (2018) Effects of d-galactose-induced ageing on the heart and its potential interventions. J Cell Mol Med 22(3):1392–1410. https://doi.org/10.1111/jcmm.13472
21. Shwe T, Pratchayasakul W, Chattipakorn N, Chattipakorn SC (2018) Role of D-galactose-induced brain aging and its potential used for therapeutic interventions. Exp Gerontol 101:13–36. https://doi.org/10.1016/j.exger.2017.10.029
22. Hsieh HM, Wu WM, Hu ML (2009) Soy isoflavones attenuate oxidative stress and improve parameters related to aging and Alzheimer's disease in C57BL/6J mice treated with D-galactose. Food Chem Toxicol 47(3):625–632. https://doi.org/10.1016/j.fct.2008.12.026
23. Offenburger SL, Ho XY, Tachie-Menson T, Coakley S, Hilliard MA, Gartner A (2018) 6-OHDA-induced dopaminergic neurodegeneration in Caenorhabditis elegans is promoted by the engulfment pathway and inhibited by the transthyretin-related protein TTR-33. PLoS Genet 14(1):e1007125. https://doi.org/10.1371/journal.pgen.1007125

24. Turgut NH, Mert DG, Kara H, Egilmez HR, Arslanbas E, Tepe B, Gungor H, Yilmaz N, Tuncel NB (2016) Effect of black mulberry (Morus nigra) extract treatment on cognitive impairment and oxidative stress status of D-galactose-induced aging mice. Pharm Biol 54(6):1052–1064. https://doi.org/10.3109/13880209.2015.1101476
25. Meng X, Chu G, Yang Z, Qiu P, Hu Y, Chen X, Peng W, Ye C, He FF, Zhang C (2016) Metformin protects neurons against oxygen-glucose deprivation/reoxygenation -induced injury by down-regulating MAD2B. Cell Physiol Biochem 40(3–4):477–485. https://doi.org/10.1159/000452562
26. Schurman LD, Carper MC, Moncayo LV, Ogasawara D, Richardson K, Yu L, Liu X, Poklis JL, Liu QS, Cravatt BF, Lichtman AH (2019) Diacylglycerol lipase-alpha regulates hippocampal-dependent learning and memory processes in mice. J Neurosci 39(30):5949–5965. https://doi.org/10.1523/JNEUROSCI.1353-18.2019
27. Zhang X, Bai L, Zhang S, Zhou X, Li Y, Bai J (2018) Trx-1 ameliorates learning and memory deficits in MPTP-induced Parkinson's disease model in mice. Free Radic Biol Med 124:380–387. https://doi.org/10.1016/j.freeradbiomed.2018.06.029
28. Fernandez SP, Muzerelle A, Scotto-Lomassese S, Barik J, Gruart A, Delgado-Garcia JM, Gaspar P (2017) Constitutive and acquired serotonin deficiency alters memory and hippocampal synaptic plasticity. Neuropsychopharmacology 42(2):512–523. https://doi.org/10.1038/npp.2016.134
29. Orr AG, Hsiao EC, Wang MM, Ho K, Kim DH, Wang X, Guo W, Kang J, Yu GQ, Adame A, Devidze N, Dubal DB, Masliah E, Conklin BR, Mucke L (2015) Astrocytic adenosine receptor A2A and Gs-coupled signaling regulate memory. Nat Neurosci 18(3):423–434. https://doi.org/10.1038/nn.3930
30. Serrano ME, Bartholome O, Van den Ackerveken P, Ferrara A, Rogister B, Plenevaux A, Tirelli E (2019) Anxiety-like features and spatial memory problems as a consequence of hippocampal SV2A expression. PLoS ONE 14(6):e0217882. https://doi.org/10.1371/journal.pone.0217882
31. Liu JH, Wang Q, You QL, Li ZL, Hu NY, Wang Y, Jin ZL, Li SJ, Li XW, Yang JM, Zhu XH, Dai YF, Xu JP, Bai XC, Gao TM (2020) Acute EPA-induced learning and memory impairment in mice is prevented by DHA. Nat Commun 11(1):5465. https://doi.org/10.1038/s41467-020-19255-1
32. Bendahmane M, Morales A, Kreutzberger AJB, Schenk NA, Mohan R, Bakshi S, Philippe JM, Zhang S, Kiessling V, Tamm LK, Giovannucci DR, Jenkins PM, Anantharam A (2020) Synaptotagmin-7 enhances calcium-sensing of chromaffin cell granules and slows discharge of granule cargos. J Neurochem 154(6):598–617. https://doi.org/10.1111/jnc.14986
33. Bacaj T, Wu D, Burre J, Malenka RC, Liu X, Sudhof TC (2015) Synaptotagmin-1 and -7 are redundantly essential for maintaining the capacity of the readily-releasable pool of synaptic vesicles. PLoS Biol 13(10):e1002267. https://doi.org/10.1371/journal.pbio.1002267
34. Xie Z, Long J, Liu J, Chai Z, Kang X, Wang C (2017) Molecular mechanisms for the coupling of endocytosis to exocytosis in neurons. Front Mol Neurosci 10:47. https://doi.org/10.3389/fnmol.2017.00047
35. Liu X, Li C, Yang Y, Liu X, Li R, Zhang M, Yin Y, Qu Y (2019) Synaptotagmin 7 in twist-related protein 1-mediated epithelial - mesenchymal transition of non-small cell lung cancer. EBioMedicine 46:42–53. https://doi.org/10.1016/j.ebiom.2019.07.071
36. Chen P, Chen F, Lei J, Li Q, Zhou B (2019) Activation of the miR-34a-mediated SIRT1/mTOR signaling pathway by urolithin A attenuates D-galactose-induced brain aging in mice. Neurotherapeutics 16(4):1269–1282. https://doi.org/10.1007/s13311-019-00753-0
37. Zhuang K, Huang C, Leng L, Zheng H, Gao Y, Chen G, Ji Z, Sun H, Hu Y, Wu D, Shi M, Li H, Zhao Y, Zhang Y, Xue M, Bu G, Huang TY, Xu H, Zhang J (2018) Neuron-specific menin deletion leads to synaptic dysfunction and cognitive impairment by modulating p35 expression. Cell Rep 24(3):701–712. https://doi.org/10.1016/j.celrep.2018.06.055
38. Ren QG, Gong WG, Zhou H, Shu H, Wang YJ, Zhang ZJ (2019) Spatial training ameliorates long-term Alzheimer's disease-like pathological deficits by reducing NLRP3 inflammasomes in PR5 mice. Neurotherapeutics 16(2):450–464. https://doi.org/10.1007/s13311-018-00698-w
39. Zhao W, Xu Z, Cao J, Fu Q, Wu Y, Zhang X, Long Y, Zhang X, Yang Y, Li Y, Mi W (2019) Elamipretide (SS-31) improves mitochondrial dysfunction, synaptic and memory impairment induced by lipopolysaccharide in mice. J Neuroinflammation 16(1):230. https://doi.org/10.1186/s12974-019-1627-9
40. Fei Z, Gao W, Xie R, Feng G, Chen X, Jiang Y (2019) Synaptotagmin-7, a binding protein of P53, inhibits the senescence and promotes the tumorigenicity of lung cancer cells. Biosci Rep 39 (2)https://doi.org/10.1042/BSR20181298
41. Luo Y, Yu Y, Zhang M, He H, Fan N (2020) Chronic administration of ketamine induces cognitive deterioration by restraining synaptic signaling. Mol Psychiatry. https://doi.org/10.1038/s41380-020-0793-6
42. Ge Y, Tian M, Liu L, Wong TP, Gong B, Wu D, Cho T, Lin S, Kast J, Lu J, Wang YT (2019) p97 regulates GluA1 homomeric AMPA receptor formation and plasma membrane expression. Nat Commun 10(1):4089. https://doi.org/10.1038/s41467-019-12096-7
43. Zhang T, Pang P, Fang Z, Guo Y, Li H, Li X, Tian T, Yang X, Chen W, Shu S, Tang N, Wu J, Zhu H, Pei L, Liu D, Tian Q, Wang J, Wang L, Zhu LQ, Lu Y (2018) Expression of BC1 impairs spatial learning and memory in Alzheimer's disease via APP translation. Mol Neurobiol 55(7):6007–6020. https://doi.org/10.1007/s12035-017-0820-z